Characterization of Current Transformers for Impedance Measurements in Automotive Immunity Test Setups

Seyyed Ali Hassanpour Razavi, Stephan Frei
TU Dortmund University
Dortmund, Germany
seyyed-ali.hassanpour-razavi@tu-dortmund.de

***Abstract* — The most commonly used automotive immunity test methods are described in the ISO 11452 series. The bulk current injection (BCI) and absorber line shielded enclosure (ALSE) apply different coupling mechanisms to assess the immunity of a device under test (DUT). The correlation between these methods is often poor, in spite of using the same cable harness and loads. It can be improved by enforcing the equivalence between the currents injected into the terminal units attached to both harness ends. Such procedure requires knowledge about the impedance at each harness end, which is directly associated with the impedance at any position along a test harness (loop impedance). Estimating the loop impedance using a RF current transformer (CT) proves to be a practical approach, due to the simple application without the need for major modifications of the test setup. In this paper, first in accordance to the lumped element model, the transformation phenomena including the input impedance, the transfer impedance, and the insertion impedance are derived. Furthermore, a wide band modelling procedure for CTs based on de-embedding a calibration fixture is developed, which provides an individual dataset suited for extracting the transformation properties and allows the expansion of the application for the impedance measurement. By focusing on the sensitivity of the input impedance as a primary quantity for measuring the loop impedance, pros and cons of using typical EMC current probes for the impedance measurement are assessed experimentally.**

Keywords—BCI; current probe; ferrite bead; impedance measurement; S- and Z-parameters; transfer impedance; insertion impedance

I. INTRODUCTION

ISO 11452-2 (ALSE-[1]) and ISO 11452-4 (BCI-[2]) are the two most common test procedures, where the electromagnetic energy is coupled in different ways to the test harness. While the ALSE method requires an anechoic chamber with high power amplifiers, demands to the BCI are much lower. Due to this reason the BCI is often used as the substitute for the ALSE. Unfortunately, the correlation of the BCI to the ALSE is often low. In order to increase the correlation between these test methods, several investigations have been published [3-5], which report different complexities and limitations concerning this issue. Enforcing the equivalence between the field coupling and the current injection either by involving two BCI probes as described in [6] or by adjusting the injected power level and proper positioning of the BCI probe along the test harness [7] (feeding and positioning conditions), greatly emphasize the importance of knowledge about the impedance of terminal unites at harness ends, namely the DUT, the load simulator, or the artificial network.

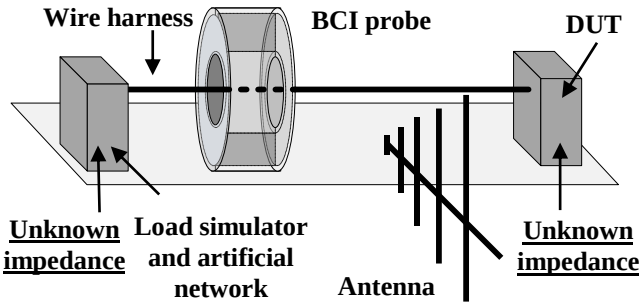

Fig. 1: General structure of automotive immunity test setups based on [1] and [2]

The termination impedances may be obtained in a direct measurement, nevertheless disconnecting the wire harness from the terminating circuit means additional preparation time and might cause problems to the proper system function. Thus, applying a toroidal CT, e.g. the BCI probe, for the indirect measurement of the impedance could be a convenient method. In [8], several methods are described for measuring the impedances indirectly with different commercial current probes. This paper extends the above-mentioned investigations by focusing on the physical analysis and the circuit implementation of the transformation phenomenon. Indications on the feasibility strength and weaknesses of using different commercial probes for the impedance measurement are given.

In line with the idea of indirect impedance measurement, the loop impedance can be considered as the entire impedance attached to the clamped conductor terminals (primary). However, from another perspective, according to the transmission line theory the loop impedance at any point along the harness is the accumulated transformed impedance of the termination circuitries at both harness ends. The measured impedance is significantly affected by the transfer function of the employed CT, which must be eliminated from the measurement by a de-embedding procedure [8]. Although a

978-1-5090-1416-3/16/$31.00 ©2016 IEEE

simple circuit model of an ideal CT appears to be sufficient for operation at lower frequency range, significant deviations from the ideal transformer operation occur at higher frequencies, which are originated from various effects such as core losses or different stray capacitances between metallic surfaces [9-11]. Consequently, to improve the impedance measurement and to figure out other properties, such as the loading effect or the transfer impedance, the characterization in a setup as close as possible to the final probe application is evident. Altogether, investigation in this paper is carried out for a CT clamped over a single wire. However, it should be recognized, that in case of a multi-wire harness, the actual impedance faced by the interference source is a highly complex combination of common and differential mode impedances at each harness end. In this paper, a BCI injection probe (FCC-F140), a commercial current probe (FCC-F65), and a self-made current transformer (SCT) composed of a ferrite bead from Wuerth-Electronics (NiZn 74271222) complemented with a single winding are selected as exemplary CTs for the comparison. In section II, a lumped circuit model is proposed to formulate the fundamental equations describing the basic operation of a CT. Section III comprises an accurate modelling procedure and the subsequent extraction of the input impedance, the transfer impedance and the insertion impedance from the model. Finally, in section IV, the sensitivity of the probes for the impedance measurement is analyzed and validated for an exemplary test setup.

II. THEORETICAL BACKGROUND OF TRANSFORMERS

A common CT is composed of a split ferrite ring with a single or multiple windings around one half to form the secondary winding of transformer. The clamped conductor forms the primary winding. Understanding the CT operation can be made easier by using an equivalent circuits. An ideal transformer considers a transformer with no losses. This means that the windings are purely inductive and the core is loss free. In an ideal transformer the impedance transformed from the primary terminals to the secondary side is

$$Z_{in} = \left(\frac{N_s}{N_p}\right)^2 Z_{loop} \xrightarrow{N_s=N_p=1} Z_{in} = Z_{loop}, \qquad (1)$$

where Z_{loop} is the impedance attached to the primary terminals and N_p and N_s are the number of windings at the primary and secondary side, respectively. Although simplified, (1) demonstrates the apparent impedance available due to transformation act by any CT. A better approximation for the probe's operation can be achieved, if a more detailed equivalent circuit is considered (see Fig. 2). The total resistor ($R_s = R_{cl}||R_{add}$) between the secondary terminals includes the core losses and an additional built-in resistor R_{add}, which may be available due to the design purposes [9]. To simplify the understanding, the capacitive coupling between different metallic components is ignored in the first step. The input port of the CT is the only directly accessible port of the system, where the measurement instrument can be connected. According to Fig. 2, the input impedance Z_{in} is the result of a parallel circuit consisting of two main branches. The first branch contains the transformed impedance due to the mutual inductance, in series with the self-inductance of the secondary side. The second branch contains the resistive component R_s.

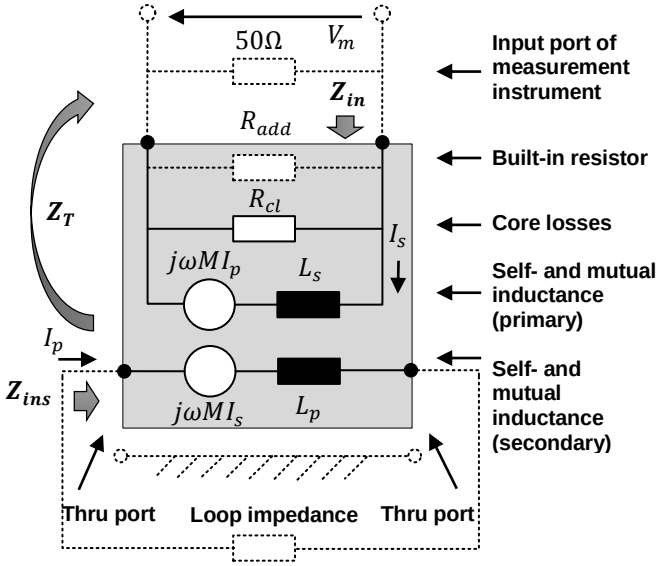

Fig. 2: A simplified circuit model for a current transformer attached to a measurement instrument with 50 Ω input impedance

Therefore, the inverse of input impedance at the input port is

$$\frac{1}{Z_{in}} = \frac{Z_{loop} + j\omega L_P}{j\omega L_s Z_{loop} - \omega^2(1-k^2)L_s L_p} + \frac{1}{R_s}, \qquad (2)$$

where k indicates the coupling coefficient between the windings ($0 \leq k \leq 1$). The chosen representation of (2) shows the restriction of the measured input admittance to the values in the range or larger than $1/R_s$, in spite of the relative complex trend of the first branch. The capacitive coupling to the secondary terminals can strengthen this effect at higher frequencies. This underlines the significance of the resistive component, as it reduces the sensitivity of the impedance measurement at the secondary side to the impedance changes at the primary terminals.

The second important parameter representing the interaction of a CT with the test setup is the insertion impedance Z_{ins}, which is defined as the impedance appearing in series with the conductor under test (the primary), when the CT is located at desired place [10]. The CT and the clamped conductor are considered as a combined network, and therefore, the insertion impedance includes the total impedance available at this location along the wire. The aforementioned assumption is valid as long as the propagation effects for the clamped conductor and the coupling between the CT and the unclamped section are negligible. As commonly used current- or BCI probe are toroidal transformers, the transformation act is bilateral and therefore, it transforms the secondary impedance into the primary as well. Based on (1), a rough estimation can be made for the input impedance. For instance, the input impedance for an ideal CT with more than 8 turns of winding at the secondary side and a 50 Ω load is approximately less than 1 Ω, which is an acceptable value for the most of applications. The application of a probe with a high insertion impedance alters the primary current considerably and may lead to unrealistic test results [10]. Considering the equivalent circuit in Fig. 2 the insertion impedance or the loading effect of a CT is the result of two

dominant parameters [11]. The secondary impedance reflected into the primary by transformation and the intrusion impedance resulted from the introduction of a magnetic core material inside the primary circuit

$$Z_{ins} = \frac{(\omega M)^2}{R + j\omega L_s} + j\omega L_p, \tag{3}$$

where *R* comprises all resistive elements in parallel at secondary side, which includes the 50 Ω input impedance of the measurement instrument. The equation (3) shows that the insertion impedance can't be eliminated by increasing the impedance connected to the secondary side in the actual test setup, since the measurement instrument often terminates the secondary terminals with 50 Ω resistor. In addition, according to (3), the insertion impedance would merely increase the characteristic impedance at this location. Nevertheless, at higher frequencies, the characteristic impedance is dominated by the capacitive coupling. The transfer impedance Z_T is defined as the ratio of the voltage developed across the output of the probe to the current in the conductor under test [10], which is derived for the proposed model in Fig. 2 and approximated for higher frequencies

$$Z_T = \frac{V_m}{I_p} = \frac{M}{L_p} \cdot \frac{j\omega L_s R_s \cdot 50}{j\omega L_s (R_s + 50) + 50 R_s} \tag{4}$$

$$\xrightarrow{approx.\ for\ HF} Z_T = \frac{M}{L_p} \cdot \frac{50 R_s}{(R_s + 50)}. \tag{5}$$

In general, current probes are designed to provide a flat frequency response over a certain frequency band. To obtain the maximum sensitivity for measuring the current, the transfer impedance should be as high as possible. The common value for the transfer impedance is between 0.1 Ω and 5 Ω [10].

III. Measurement Based Modelling And Estimation of Different Probe's Properties

Although the representation of CTs in terms of the lumped circuit model is acceptable for describing various properties in the lower frequency range, a more accurate model is required to cover the spectral content at higher frequencies. A three-port network model proves to be an appropriate modelling method for this purpose, where the probe's connector (input port) and both terminals between the conductor and ground plane, the so called 'thru port', represent the three ports of the network. Since both thru ports aren't accessible directly, in a setup similar to actual application of probe, the three-port S-parameter-set is recorded and the impact of the measurement setup is de-embedded from original dataset subsequently. As illustrated in Fig. 3, a straight single-wire of 30 cm is spanned within two vertical L-form fixtures in 50 mm over a copper ground plane. Two SMA adaptors are used for the transition to the measuring cables to make the other two ports accessible to the measuring device. The setup can be interpreted as three separate modules: a two-port network on the left (fixture and single wire), a three-port central module (CT and the clamped wire), and a two-port network on the right. The single wire and test fixtures are characterized in advance and therefore, are considered together as a two-port network with a known S-parameter matrix.

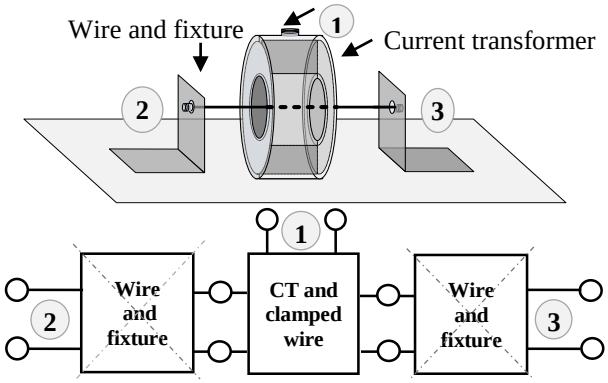

Fig. 3: Calibration setup for extracting the three-port model, de-embedding wire and fixture from the three-port S-parameter measurement

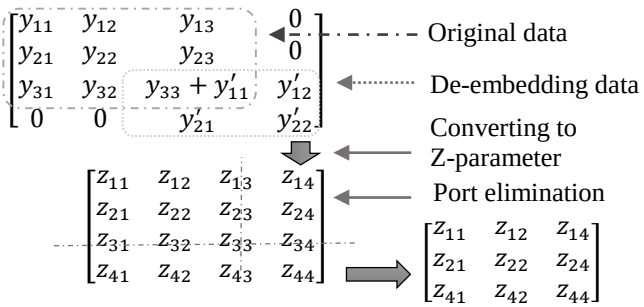

Fig. 4: Mathematical procedure for de-embedding the wire-fixture dataset from the right side of the three-port dataset and removing the superfluous port

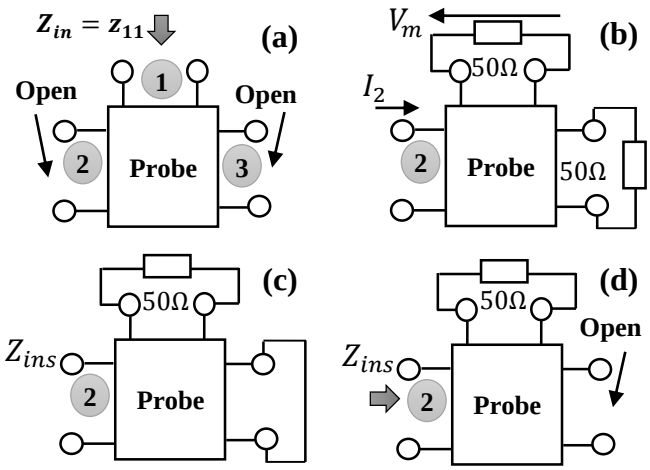

Fig. 5: Application of the 3-port dataset to determine different probe's properties input impedance (a), transfer impedance (b), and insertion impedance (c-d)

However, in case of three ports, the matrix multiplication in terms of the T-parameter is not possible. Therefore, first, the chain matrix (ABCD-parameter) of the redundant two-port dataset is inverted, to obtain a dataset for the de-embedding. However, from the network point of view, the impact of a superfluous port remains in the dataset in such cascading process. A straightforward approach to eliminate this port is to leave the port open by converting the resulted 4-by-4 matrix to Z-parameter and removing all related entries from the matrix. The remaining three-port dataset involves the frequency response of the setup with the wire-fixture structure removed from right side. This process is repeated for the wire-fixture

structure on the other side by rearranging the original dataset to the appropriate order to obtain a model, which contains the probe's frequency response. In order to determine the different characteristics of the SCT, the BCI probe, and the current probe three individual models are extracted from the three-port S-parameter datasets measured with an Agilent E601B network analyzer between 300 kHz and 1 GHz.

A. *Estimation of Input Impedance*

Based on the extracted three-port model, the input impedance in absence of the primary winding is simulated by leaving both thru ports open (see Fig. 5-a). The simulation results for the input impedance magnitude, plus the positive real and imaginary part of the complex value are illustrated in Fig. 6-a. The trend for the inductive and resistive regions follow the expected behavior of ferrite cores with different relative permeabilities. Fitting the complex impedance value to (2), estimates different parameters, such as the self-inductance and the resistive elements at the secondary side. In case of the current probe a flat real part can only be reached with a sufficiently small additional built-in resistor. Additionally, the significant inductive behavior corresponds to the anticipated length of the wire and probe's connector. Moreover, the length and width of the secondary winding of the BCI probe (more than 12 cm) leads to a noticeable propagation effects at higher frequencies.

B. *Estimation of Transfer Impedance*

Typical current monitoring probe data sheets provide merely the magnitude of transfer impedance measured in a standard calibration fixture. To reduce calibration errors and maximize the measurement accuracy, the calibration is generally performed in a 50 Ω end to end system, which minimizes the VSWR at the input of the fixture. However, in accordance with the definition of transfer impedance, the complex value can be calculated from the extracted three-port model. According to Fig. 5-b, the current flowing into the second port I_2 for a known forward power P_{Fwd} can be calculated

$$I_2 = (1 - s_{22})\sqrt{\frac{P_{Fwd}}{Z_0}}, \tag{6}$$

where s_{22} is the reflection at port 2 with the reference impedance Z_0. The induced voltage at the port 1 for a certain forward power is given by

$$V_m = s_{12}\sqrt{P_{Fwd} \cdot Z_0}. \tag{7}$$

Therefore, the transfer impedance of the probe is calculated based on its definition as follows

$$Z_T = \frac{V_m}{I_p} = Z_0 \frac{s_{21}}{1 - s_{11}}. \tag{8}$$

The simulation results in Fig. 6-b confirms the expected constant transfer impedance for a wide frequency range. Although having an unsteady transfer impedance value, both BCI probe and the SCT point out more sensitivity to the current changes at the primary side, which can be used for the current measurement by accepting the undesirable effects introduced into the circuit described hereafter.

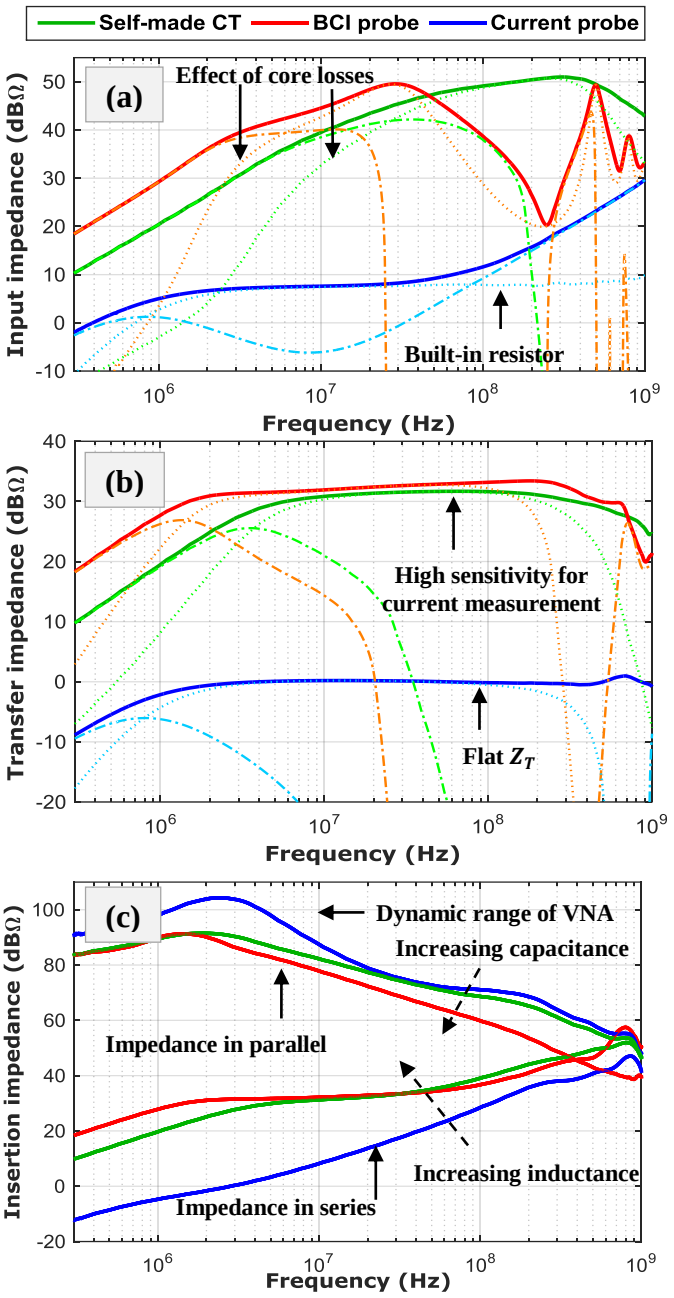

Fig. 6: Extracted impedance magnitude for input impedance (a), transfer impedance (b) and insertion impedance (c). Real part (-·-) and imaginary part (-··-) are demonstrated for the complex value of the extracted impedances.

C. *Estimation of Insertion Impedance*

Estimation of the impedance in series with current flow is carried out from the three-port network by an appropriate termination of port 2 and 3 virtually and simulating the one-port reflection measurement at port 1 (see Fig. 5-c). For this purpose, the network is terminated with a 50 Ω resistor emulating the standard port of the measurement instrument. In addition, the terminals of the port 3 are shortened to create a closed loop at the primary side. However, the impact of the discontinuity, particularly in case of the BCI-probe (7 cm) cannot be considered as a mere impedance in series with the wire under

test. The extracted insertion impedance in Fig. 6-c shows that the BCI probe and the SCT contribute to a considerable higher impedance in series to the test harness in comparison to the current probe. From other perspective, in order to assess the capacitive coupling, in a similar approach, the parallel impedance to the ground resulted from the probe's conductive structure can be estimated by terminating the input port with a 50 Ω and leaving the port 3 open (see Fig. 5-d).

IV. Measuring Loop Impedance with Different Probes

With respect to the considerations in section I, an accurate estimation of the loop impedance as a primary quantity correlating to the impedances at the harness ends is from considerable importance. The aim here is to assess the feasibility, strength and weaknesses of applying the aforementioned probes for the impedance measurement. In order to measure the loop impedance by means of a CT indirectly, several approaches are proposed in [8]. A straightforward method is to remove the frequency response of the CT from a reflection measurement (one-port S-parameter measurement) with a VNA, which is equivalent to connect the VNA measuring port directly to the loop impedance. For this purpose, the extracted three-port dataset $[S]_{3x3}$ (single-ended) is converted to a two-port dataset $[S']_{2x2}$ composed of a single-ended port (input port) and a differential port representing both thru ports

$$s'_{11} = s_{11}, \qquad s'_{22} = \frac{1}{2}\,(s_{22} - s_{23} - s_{32} + s_{33}) \tag{9}$$

$$s'_{12} = \frac{1}{\sqrt{2}}\,(s_{12} - s_{13}), \qquad s'_{21} = \frac{1}{\sqrt{2}}\,(s_{21} - s_{31}). \tag{10}$$

Multiplication of the inverse T-parameter of the two-port dataset with the T-parameter of the reflection measurement result in the T-parameter of the load attached to the primary terminals. If the load is connected directly between both thru ports, such inversion procedure for a test setup is prone to small errors. This is resulted from the lack of the similarity between the calibration and the application test setup. Furthermore, as stated by 2, the parallel resistive elements act as the upper bound for the measured input impedance. Mapping the entire domain of the loop impedance into a small codomain restricted to a low impedance, degrades the quality of the primary measurement and may lead to the total failure of the de-embedding procedure. A possible solution to mitigate the de-embedding problems is to choose a CT with better impedance transformation characteristic, i.e. higher sensitivity to the impedance changes at the primary side.

A. *Sensitivity of Probes to Impedance Changes at Primary Side*

The sensitivity for the aforementioned CTs is evaluated in a brute force method by simulating the corresponding input impedance for two extreme cases connected to the primary terminals, i.e. the open- and short circuits. The simulation results in Fig. 7 indicate a significant gap between the open- and short circuits in case of the self-made CT and the BCI probe. Conversely, the current probe remains almost insensitive throughout the entire frequency range. This means that the entire range of possible impedances at the primary side is mapped to a very small region which may not be identifiable by VNA.

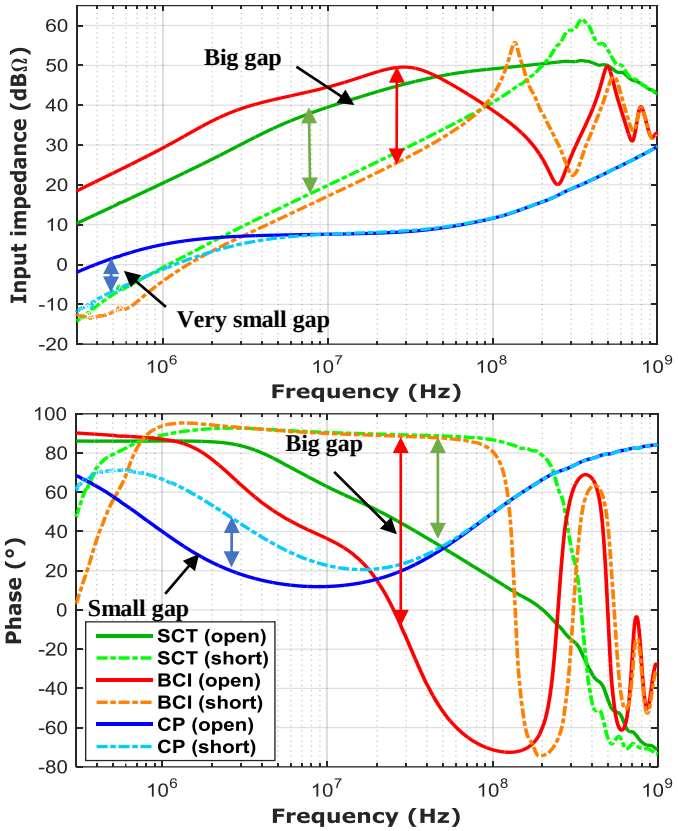

Fig. 7: Magnitude and phase of the simulated input impedance for the open- and short circuits at the primary side to reveal the sensitivity of self-made CT (SCT), BCI probe (BCI), and current probe (CP)

B. *Application for Indirect Loop Impedance Measurement*

In order to apply the de-embedding process to measure the loop impedance indirectly, a setup similar to the calibration structure with a different length (1 m) is realized (see Fig. 8). The ports 2 and 3 are terminated with 50 Ω SMA-resistors. The one-port S-parameter is recorded by positioning each CT in the middle of the structure. The estimated results for the loop impedance after de-embedding the CT's frequency response is demonstrated in Fig. 9. The estimated loop impedance with the SCT and the BCI corresponds to the expected impedance value in the middle of the structure. In contrast, measuring the loop impedance with the current probe leads to incorrect results.

V. Discussion and Conclusions

In this paper, the characterization procedure of current transformers to expand their application for impedance measurement was addressed. To this end, a theoretical framework for a better understanding and interpretation of the transformation phenomena is presented and discussed. The impact of the common physical properties of the current transformers and individual designed-based modifications on three principal properties, namely the input impedance, the transfer impedance, and the insertion impedance is investigated.

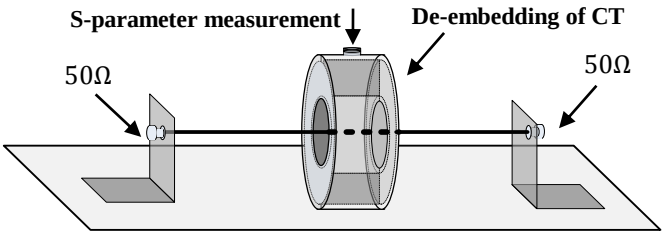

Fig. 8: Experimental setup for validation of indirect impedance measurement.

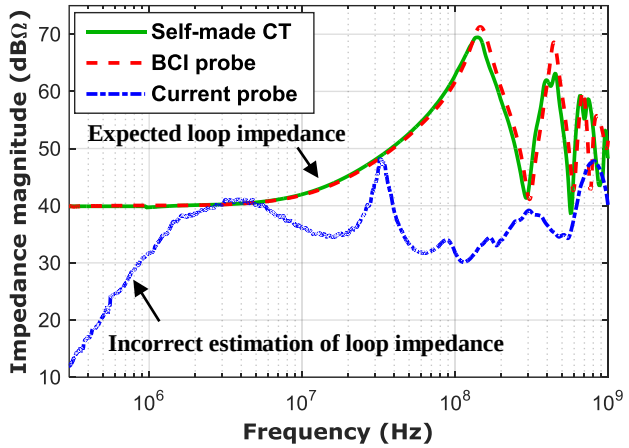

Fig. 9: Estimated results for the loop impedance after de-embedding the current transformer from direct S-parameter measurement.

Although the modelling procedure based on the S-parameter measurement requires a de-embedding dataset for the redundant structure (wire-fixture), the user is exempt from having knowledge about the internal structure and the physical properties of the CT. Furthermore, such modelling procedure overcome the complexities related to the lumped circuit modelling at higher frequencies.

From the stand point of impedance measurement, the input impedance turned out to be a key and primary quantity for any further analysis. Hence the proposed input impedance assessment was targeted to analyze the sensitivity of different CTs to the impedance changes at the primary side. From the stand point of insertion impedance, it was shown that current probe (FCC F-65) has the least loading effect on the clamped conductor, whereas the BCI probe and the self-made CT affect the test harness significantly. However, according to the sensitivity analysis and the corresponding de-embedding procedure, only the self-made CT and the BCI probe are suited for the impedance measurement up to 1 GHz. Failure of the de-embedding procedure in case of the current probe, makes this probe definitely unemployable for the impedance measurement purposes. In consequence, the impedance measurement can be improved by employing a CT with less core losses and less parasitic capacitive coupling to the environment in order to approach the conditions in (1). The very small dimensions of the CT (in comparison to the shortest expected wavelength) and the higher dynamic range of measurement instrument by averaging or reducing the IF bandwidth of VNA increase the measurement quality significantly. Improving the correlation between the ALSE and the BCI as the primary goal of this research, requires the impedance on both ends of the test harness, which can be estimated with at least two measurement at different positions along the harness.

However, two main difficulties are stand in the way:

1. The overall accuracy of the de-embedding procedure is strictly related to the matching between the calibration and the measurement setup and the exact separation between the wire-fixture and the CT network model.
2. All investigations described here refer to a single-wire and serve as a primary research, which should be extended to the practically relevant case of multi-wire harness.

On the whole, the proposed methods are aimed to highlight the potential of the measurement-based modelling of current transformers and extend their application for indirect impedance measurement.

References

[1] ISO 11452-2: Road vehicles - Component test methods for electrical disturbances from narrowband radiated EM energy -- Part 2: Absorber-lined shielded enclosure.

[2] ISO 11452-4: Road vehicles-component test methods for electrical disturbances from narrowband radiated EM energy, Part 4: Bulk Current Injection.

[3] J.W. Adams, J. Cruz, and D. Melquist, "Comparison measurements of currents induced by radiation and injection," IEEE Trans. Electromagn. Compat., vol. 34, no. 3, pp. 360–362, Aug. 1992.

[4] D.A. Hill, "Currents induced on multiconductor transmission lines by radiation and injection," IEEE Trans. Electromagn. Compat., vol. 34, no. 4, pp. 445–450, Nov. 1992.

[5] S. Pignari and F.G. Canavero, "Theoretical assessment of bulk current injection versus radiation," IEEE Trans. Electromagn. Compat., vol. 38, no. 3, pp. 469–477, Aug. 1996.

[6] F. Grassi, G. Spadacini, F. Marliani, S.A. Pignari, "Use of Double Bulk Current Injection for Susceptibility Testing of Avionics," IEEE Trans. Electromagn. Compat., vol. 50, vo. 3, pp. 524-535, Aug. 2008.

[7] S.A. Hassanpour Razavi, S. Miropolsky, S. Frei, "Verbesserung der Korrelation zwischen dem BCI- und dem Antennenprüfverfahren für Kfz-Komponenten durch Anpassung von Verstärkerleistung und Position der BCI-Zange," EMV-Düsseldorf, Germany, 2014

[8] S.A. Hassanpour Razavi, A. Zeichner, S. Frei, "Erhöhung der Korrelation zwischen BCI- und Antennenprüfverfahren durch Bestimmung von Abschlussimpedanzen mittels potenzialfreier Messung mit Stromsensoren," EMV-Düsseldorf, Germany, 2014

[9] D. C. Smith, "Current Probes, More Useful Than You Think," IEEE Int. Symp. EMC, Denver, pp. 284-289, Aug. 1998.

[10] International Electrotechnical Commission – International Special Committee on Radio Interference, "CISPR 16-1-2, Part 1-2: Radio disturbance and immunity measuring apparatus – Ancillary equipment – Conducted disturbances"

[11] C.F.M. Carobbi and L.M. Millanta, "The Loading Effect of Radio-Frequency Current Probes," IMTC 2006, Italy, Apr. 2006